

Contents lists available at [SciVerse ScienceDirect](#)

## Radiotherapy and Oncology

journal homepage: [www.thegreenjournal.com](http://www.thegreenjournal.com)

## Original article

## TP53 induced glycolysis and apoptosis regulator (TIGAR) knockdown results in radiosensitization of glioma cells

Miguel A. Peña-Rico<sup>a,1</sup>, María Nieves Calvo-Vidal<sup>a,1</sup>, Ruth Villalonga-Planells<sup>b</sup>, Fina Martínez-Soler<sup>b</sup>, Pepita Giménez-Bonafé<sup>b</sup>, Àurea Navarro-Sabaté<sup>a</sup>, Avelina Tortosa<sup>b,c</sup>, Ramon Bartrons<sup>a</sup>, Anna Manzano<sup>a,\*</sup><sup>a</sup>Unitat de Bioquímica; <sup>b</sup>Unitat de Fisiologia, Dept. Ciències Fisiològiques II; and <sup>c</sup>Department IMQ, Campus de Ciències de la Salut, Institut d'Investigació Biomèdica de Bellvitge-Universitat de Barcelona, Spain

## ARTICLE INFO

## Article history:

Received 3 November 2010

Received in revised form 4 July 2011

Accepted 7 July 2011

Available online xxxxx

## Keywords:

TIGAR

Radiotherapy

Oxidative stress

Senescence

DNA repair

## ABSTRACT

**Background and purpose:** The TP53 induced glycolysis and apoptosis regulator (TIGAR) functions to lower fructose-2,6-bisphosphate (Fru-2,6-P<sub>2</sub>) levels in cells, consequently decreasing glycolysis and leading to the scavenging of reactive oxygen species (ROS), which correlate with a higher resistance to cell death. The decrease in intracellular ROS levels in response to TIGAR may also play a role in the ability of p53 to protect from the accumulation of genomic lesions. Given these good prospects of TIGAR for metabolic regulation and p53-response modulation, we analyzed the effects of TIGAR knockdown in U87MG and T98G glioblastoma-derived cell lines.

**Methods/results:** After TIGAR-knockdown in glioblastoma cell lines, different metabolic parameters were assayed, showing an increase in Fru-2,6-P<sub>2</sub>, lactate and ROS levels, with a concomitant decrease in reduced glutathione (GSH) levels. In addition, cell growth was inhibited without evidence of apoptotic or autophagic cell death. In contrast, a clear senescent phenotype was observed. We also found that TIGAR protein levels were increased shortly after irradiation. In addition, avoiding radiotherapy-triggered TIGAR induction by gene silencing resulted in the loss of capacity of glioblastoma cells to form colonies in culture and the delay of DNA repair mechanisms, based in  $\gamma$ -H2AX foci, leading cells to undergo morphological changes compatible with a senescent phenotype. Thus, the results obtained raised the possibility to consider TIGAR as a therapeutic target to increase radiotherapy effects.

**Conclusion:** TIGAR abrogation provides a novel adjunctive therapeutic strategy against glial tumors by increasing radiation-induced cell impairment, thus allowing the use of lower radiotherapeutic doses.

© 2011 Elsevier Ireland Ltd. All rights reserved. Radiotherapy and Oncology xxx (2011) xxx–xxx

TIGAR (TP53 induced glycolysis and apoptosis regulator) has been identified as an early target of p53. By lowering the levels of fructose-2,6-bisphosphate (Fru-2,6-P<sub>2</sub>), TIGAR redirects glucose into the pentose phosphate pathway (PPP) enhancing NADPH production and increasing the capacity of cells to handle redox stress, thereby protecting them from apoptosis [1]. Recently Li et al. made a structural analysis of TIGAR demonstrating that the TIGAR structure forms a histidine phosphatase fold and has an active site with bisphosphatase activity [2], which leads to reduced Fru-2,6-P<sub>2</sub> levels. This metabolite is a key regulator of glycolysis and its concentration depends on the activity of different bifunctional enzymes called 6-phosphofructo-2-kinase/fructose-2,6-bisphosphatase (PFK-2/FBPase-2) encoded by four genes (PFKFB1–4) [3]. In particular, it is known that the transcription of PFKFB3 is modulated by HIF-1 (Hypoxia Inducible Factor-1) and upregulated in cancer, hence the synthesis and elimination of Fru-2,6-P<sub>2</sub> by PFKFB3 and

TIGAR are controlled by HIF-1 and p53 respectively, which points out to the relevance of metabolic regulation for tumor suppression [4].

The importance of TIGAR as a regulator of oxidative stress is reflected in its capacity to modulate apoptosis, autophagy and senescence [1,5,6]. ROS regulate several cellular processes, although at higher levels they can induce genotoxic damage and cell death [7]. Indeed, an imbalance between ROS generation and elimination can contribute to disease development, such as cancer. In this context, oxidative stress is a condition that glioblastoma multiforme (GBM) cells encounter in the necrotic zone, which is one of the stressful conditions that GBM cells need to withstand in order to survive [8]. GBM is the most aggressive primary brain tumor in adults; its hallmark features are uncontrolled proliferation, diffuse infiltration, propensity to necrosis, robust angiogenesis, intense resistance to apoptosis and genomic instability [9]. Following surgery or biopsy, radiotherapy, often in conjunction with adjuvant chemotherapy, modestly improves survival, although glioma cell resistance to radiotherapy remains a major obstacle [10,11].

A number of studies have identified several molecular mechanisms of glioma cell radioresistance [12]. Despite these advances,

\* Corresponding author. Address: Unitat de Bioquímica, Universitat de Barcelona, Feixa Llarga s/n, E-08907 L'Hospitalet, Barcelona, Spain.

E-mail address: [annamanzano@ub.edu](mailto:annamanzano@ub.edu) (A. Manzano).

<sup>1</sup> These authors equally contributed to this work.

a significant clinical improvement has not been achieved. Therefore, an exhaustive characterization of the molecular mechanisms of resistance is necessary in order to uncover targets for novel therapies. One potential basis for radiosensitivity is through differences in ROS levels, which are involved in radiation-induced damage. A critical event in determining radiosensitivity is the repair of DNA double-strand breaks (DSB) [13]. Furthermore, several authors have described the importance of glycolytic metabolism and free radicals in chemo- and radiotherapies in glioma cells. ROS levels are influenced by a number of endogenous factors [14,15], including TIGAR antioxidant activity, which increases the feeding of glucose-6 phosphate into the PPP to produce glutathione (GSH) [16,17]. A recent study has revealed that enhanced PPP and increased antioxidant capacity correlate with metastasis of breast cancer cells to the brain [18]. In addition, recent findings have demonstrated that an anticancer molecule mediates its effects via TIGAR downregulation associated with a decrease in NADPH levels [19]. In the present study, we look at the TIGAR knockdown effects in glioma U87MG and T98G cells and analyze its potential therapeutic utility as an enhancer of radiotherapy action in glioblastoma derived cell-lines.

## Materials and methods

### Cell culture

U87MG (TP53 wild-type) and T98G (TP53 mutant, M237I) human glioma cell lines were obtained from the American Type Culture Collection and cultured with DMEM with 10% fetal calf serum (FCS) supplemented with L-glutamine (2 mM) and penicillin-streptomycin (100 U/ml–100 µg/ml) in a humidified atmosphere of 5% CO<sub>2</sub>. Both cell lines were verified to be mycoplasma-free and p53 status was determined by sequencing.

### siRNA design and transfection

Small interfering RNAs (siRNAs) were designed according to criteria outlined elsewhere [20]. Specificity was checked by BLAST. Transfections were carried out using three Stealth siRNAs (Invitrogen Corp.) sequences targeted against TIGAR ("TIGAR-siRNA") (T1: 5'-GAAGUUAACCAACGGUUCAGUGUA-3', T2: 5'-CAGGAUCAUCUAAAUGGACUGACUG-3' and T3: 5'-CAAGCAGCAGCUGCGUUAUUAUUC-3') and two medium GC negative control Stealth siRNAs ("Neg-siRNA") (5'-GAAGUUAACCAACGGUUCAGUGUA-3' and 5'-CAGGAUCAUCUAAAUGGACUGACUG-3'). Cells were plated at a density of  $2.5 \times 10^5$  cells in 6-well plates and allowed to attach overnight. Cells were then transfected using Oligofectamine (Invitrogen Corp.) diluted in Opti-MEM Reduced Serum Medium (GIBCO). The final siRNA concentration was 75 nM. After 4 h, complete media was added to each well. 24 h after transfection, cells were trypsinized, resuspended in fresh media, and re-plated for clonogenic cell survival and cell viability assays.

### Irradiation

Forty-eight hours after siRNA transfection, cells were treated at room temperature with  $\gamma$ -irradiation using an  $\gamma$ -ray unit (Clinac 600 CD, M/S Varian AG) at dose-rate of 0.90 Gy/min to a total absorbed dose of 2.0, 4.0, 6.0, 8.0 and 10.0 Gy. Irradiation was undertaken at Hospital Duran i Reynals from the Applied Radiobiology and Experimental Radiotherapy Group from ICO -IDIBELL.

### Cell number assay

Cell number was determined by crystal violet staining as in Calvo et al. [21]. Cells attached to the culture plate were stained with crystal violet and, after dissolving the dye with 1% SDS, the

absorbance read at 550 nm was plotted as proportional to the cell number.

### Protein extraction and Western blot analysis

Protein was extracted from cells using SDS buffer (50 mM Tris-Cl, 1% SDS, 10% glycerol) supplemented with protease inhibitors. Protein concentration was determined by BCA protein assay (Bio-Rad). Equal amounts of total protein extracts were analyzed in 10% (w/v) SDS-PAGE. Western blot was performed [22] using a rabbit polyclonal antibody against TIGAR (1:1000) (Lifespan), and, for protein loading control, a mouse monoclonal antibody against  $\alpha$ -tubulin (1:1000) (Sigma). Peroxidase-conjugated secondary antibodies against mouse and rabbit (Amersham Bioscience) were used at 1:5000. Immunostaining was carried out using the ECL technique (Amersham-Pharmacia Biotech). Densitometric analysis was carried out using Multi-Gauge v3.0 (FujiFilm Corporation, 2007) software.

### Metabolite determination

To measure Fru-2,6-P<sub>2</sub> levels, U87MG cells were homogenized in 0.1 M NaOH containing 0.1% (v/v) Triton X-100, heated to 80 °C for 15 min, and centrifuged at 14,000g for 5 min. Fru-2,6-P<sub>2</sub> was determined in supernatants by its ability to activate pyrophosphate-dependent PFK-1 from potato tubers as described by Van Schaftingen et al. [23]. Lactate was measured spectrophotometrically in neutralized perchloric extracts by using standard enzymatic methods [24]. Protein concentration was determined by the Bradford-based Bio-Rad assay. For GSH determination U8MG cells were homogenized directly in a cold medium containing 20 mM HCl, 5 mM diethylenetriaminepentaacetic acid (DTPA), 10 mM ascorbic acid, and 5% trichloroacetic acid (TCA). Suspensions were centrifuged at 14,000g and the resulting supernatants containing GSH were collected and stored at -70 °C, whereas the pellets were washed twice, neutralized in 0.1 M NaOH, and stored at -20 °C for protein determination. Levels of GSH were determined fluorometrically using the fluorescent probe o-phthalaldehyde (OPA), as reported elsewhere [25].

### Total cellular ROS Levels

siRNA-transfected cells were incubated for 24, 48 or 72 h. After three washes with PBS, cells were loaded with the oxidative-sensitive dye 2',7'-dichlorodihydrofluorescein diacetate (H<sub>2</sub>DCFDA) by replacing the medium with phenol red-free DPBS containing 10% FBS and 10 µM H<sub>2</sub>DCFDA for 30 min at 37 °C, in a 5% CO<sub>2</sub> cell incubator. Unincorporated dye was removed by washing once with DPBS + FBS and two times with PBS, and cells were lysed with a buffer containing 25 mM Hepes pH 7.5, 1.5 mM MgCl<sub>2</sub>, 0.2 mM EDTA, 0.1% Triton X-100 and protease inhibitors. Homogenates were transferred in duplicate into a 96-well clear bottom black plate and DCF fluorescence was assayed with an excitation wavelength of 488 nm and an emission wavelength of 520 nm in a Microplate Fluorescence Reader Fluostar Optima. Results were expressed as fold change of their respective controls after correction with protein content.

### Clonogenic survival assay

Twenty-four hours after siRNA transfection,  $1 \times 10^2$  U87MG cells were plated in triplicate in 6-well plates. Plates were irradiated 48 h after transfection as described above. 14 days after irradiation, cells were fixed in 1% crystal violet (containing 30% ethanol) and visualized under an inverted phase-contrast microscope. Cells were then washed with distilled water and colonies consisting of  $\geq 50$  cells were counted as a single colony. The

relative percentage of surviving cells was calculated by dividing the number of treated cell colonies by that of the control cells [26].

#### Apoptosis analysis

Apoptotic or necrotic cells were determined by the annexin V binding assay [27]. The affinity of annexin V for phosphatidylserine residues allows the percentage of cells undergoing apoptosis to be quantified by flow cytometry. Apoptotic and necrotic cells were distinguished on the basis of double-labeling for annexin V-FITC (Bender) and propidium iodide (PI), a membrane-impermeable DNA stain. Floating and freshly trypsinized cells were pooled, washed twice in binding buffer and processed following the manufacturer's instructions. Cell fluorescence was analyzed by flow cytometry (FACS Calibur, Becton Dickinson) using the Cell Quest Pro software.

#### Senescence Associated- $\beta$ -Galactosidase (SA- $\beta$ -Gal) staining

A senescence detection kit from Biovision was used. Briefly, cells were washed in PBS and fixed with fixative solution 10–15 min at room temperature. Cells were washed twice with PBS and incubated in fixative solution containing X-Gal at 37 °C in a dark humidified chamber. Staining was evident in 12–14 h [28]. Percentage of SA- $\beta$ -Gal-positive cells was counted at 400 $\times$  magnification by examining 10 random fields under the microscope.

#### Immunofluorescent $\gamma$ -H2AX staining

Cells were fixed with 2% paraformaldehyde in PBS 30 min, 1, 4 and 24 h post-irradiation and then were immunostained for  $\gamma$ -H2AX with an Alexa-488-conjugated anti-rabbit IgG (Molecular Probes) for visualization of foci. Images of  $\gamma$ -H2AX foci and nuclei were acquired with a Spectral Confocal Microscope (TCS-SL, Leica Microsystems, Wetzlar, Germany) using a Plan-Apochromat 63 $\times$ /1.4 N.A. immersion oil objective (Leica Microsystems). We used excitation laser beam at 633 nm (Lasos Inc) and pinhole of 114.54  $\mu$ m for To-pro-3 nuclear staining, and Argon Laser at 488 nm and pinhole of 114.54  $\mu$ m for Alexa fluor 488 foci staining. Images were captured using the accompanying image processing software from Cytovision. Images of  $\gamma$ -H2AX foci and nuclei were exported separately as tif files and processed using Image J software (U.S. National Institutes of Health, <http://rsb.info.nih.gov/ij/download.html>). For U87MG and T98G cells a minimum particle size of 11.6 pixels (0.108  $\mu$ m<sup>2</sup>) and 12.59 (0.117  $\mu$ m<sup>2</sup>), respectively and threshold gray value of 20 were chosen. For each treatment condition,  $\gamma$ -H2AX foci were determined and the average number of  $\gamma$ -H2AX foci per cell nucleus from three independent experiments was plotted.

#### Statistical analysis

Results are expressed as means  $\pm$  standard error of the mean (S.E.M.) of values obtained in independent experiments. Differences between samples were analyzed with the Student's *t* test. Significant differences at *p* < 0.05, 0.01, and 0.001 versus negative control are indicated by \*, \*\*, and \*\*\*, respectively. All calculations were performed using the 14.0 SPSS software package (SPSS Inc.).

## Results

#### TIGAR expression knockdown affects glioblastoma cells metabolism and growth rate

The aim of this study was to investigate the biological consequences of the specific knockdown of TIGAR in U87MG and T98G

glioblastoma-derived cell lines. Three different siRNA molecules were designed to silence TIGAR.

Preliminary studies on protein levels showed between 60 and 80% of silencing using specific T1, T2 or T3 siRNAs and no significant differences were observed. A mix of them (T1, T2 and T3 siRNAs) was prepared to perform most of the experiments, and some experiments were performed with T1 siRNA alone. U87MG cells were transfected, 24 h post-plating, with either negative siRNA (Neg-siRNA) or TIGAR mix siRNA (TIGAR-siRNA) at 75 nM final concentration. U87MG samples were collected 24, 48 and 72 h post-transfection and TIGAR protein expression was assessed by Western blot and normalized by  $\alpha$ -tubulin. **Supplementary Fig. 1A** shows a representative time-course of TIGAR knockdown that reveals decreased levels of TIGAR 24 h after transfection, which were sustained at least for 72 h. Metabolic parameters related with TIGAR function were determined and Fru-2,6-P<sub>2</sub> and lactate levels were significantly increased in TIGAR-silenced U87MG cells 24 h after transfection (**Supplementary Fig. 1B**). Redox state was evaluated by assaying GSH and total ROS levels. The presence of ROS coincided with a decrease in GSH levels as a consequence of TIGAR knockdown. GSH basal levels decreased during the time-course, but TIGAR knockdown made that decrease more pronounced (**Supplementary Fig. 1C and D**). Subsequently, we evaluated the effect of TIGAR silencing on the growth rate of transfected U87MG cells harvested between 1 and 5 days after plating. Growth rate of Neg or TIGAR-silenced cells was monitored by crystal violet staining in a 5-day time-course. U87MG cells treated with TIGAR-siRNA (T1 or Tmix) exhibited a 25% reduction in the slope of the growth rate in comparison with control cells (**Sup Fig. 2A**). U87MG TIGAR-silenced cells show a clear reduction on cell confluence compared to negative control transfected cells. Similar results were obtained with T98G cells (**Supplementary Fig. 2B**).

#### TIGAR knockdown induces senescence in glioblastoma cells

In order to determine the mechanisms involved in the decreased growth rate, programmed cell death type I (apoptosis) and type II (autophagy) were evaluated. **Supplementary Fig. 2C and 2D** show that no significant differences were observed in apoptosis levels measured by annexin/PI staining in U87MG cells. Similar results were obtained in T98G cells when apoptosis was measured 48 h after TIGAR knockdown (**Supplementary Fig. D**). The process of autophagy was evaluated by the study of autophagy markers protein expression and no differences were observed in LC3-II levels, whereas p62 levels slightly increased, indicating that autophagy is not activated in TIGAR-silenced U87MG cells (**Supplementary Fig. 2E**). On the other hand, Senescence Associated- $\beta$ -Galactosidase (SA- $\beta$ -Gal) staining of TIGAR-knockdown U87MG and T98G cells revealed a clear increase of senescent cells. This increase in SA- $\beta$ -Gal positive cells was obtained both with the TIGAR siRNA mixture and with the T1 siRNA 1 (**Fig. 1A**).

#### TIGAR knockdown induces DNA damage

In order to estimate whether the increased ROS levels due to TIGAR silencing could be acting as a genotoxic insult, DNA damage was measured by the immunostaining of phosphorylated H2AX protein ( $\gamma$ -H2AX), which is recruited to nuclear structures termed foci. 36 h after siRNA transfection, the presence of some  $\gamma$ -H2AX foci in U87MG and T98G TIGAR-silenced cells was observed in contrast with their respective control cells.  $\gamma$ -H2AX foci were prevented by pre-incubation with butylated hydroxyanisole (BHA) (0.1  $\mu$ g/mL, 24 h), a potent ROS scavenger (**Fig. 1B and C**).

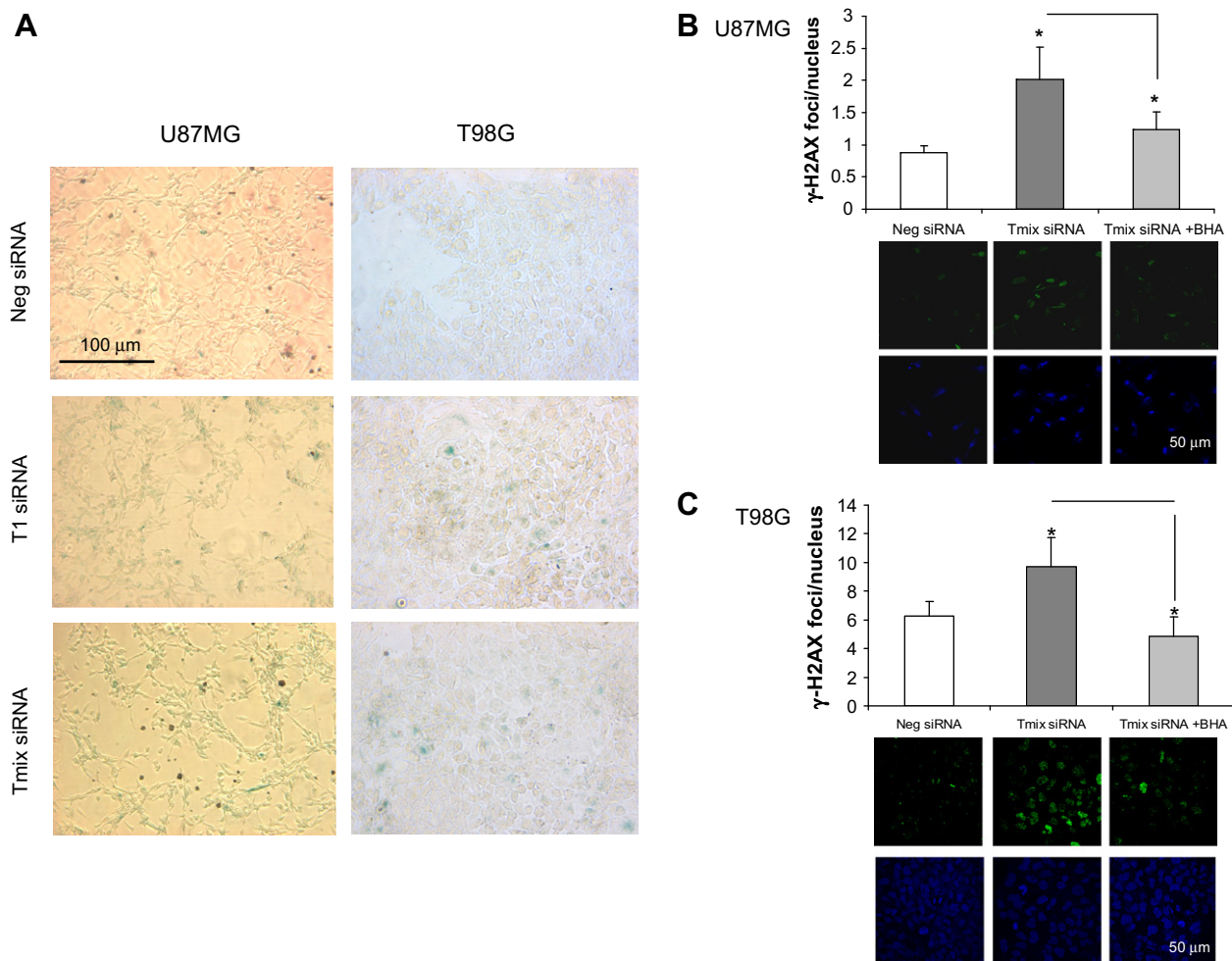


**Fig. 1.** Induced senescence and DNA damage after TIGAR knockdown on U87MG and T98G cells. (A) Representative of at least three experiments showing SA- $\beta$ -Gal activity in U87-MG and T98G cells 120 h post-transfection. (B and C) Representative immunofluorescence staining showing the focal distribution of phosphorylated H2AX in U87MG and T98G cells, respectively, 36 h post-transfection with negative (Neg) or TIGAR mix (Tmix) siRNAs. Green: phosphorylated H2AX, blue: To-pro-3 (nucleus). Some cells were pre-incubated with BHA (0.1  $\mu$ g/ml) for 24 h before staining. Bars plotted in the upper panel represent the average number of foci/cell from three experiments as determined by the use of ImageJ software; at least 300 cells were counted from 10 randomly chosen fields of view. Values are means  $\pm$  S.E.M. Student's *t* test versus TIGAR-silenced cells values: \**p* < 0.05.

#### Induction of TIGAR by radiotherapy

Radiotherapy is a conventional treatment against gliomas that generate stress and modulate gene expression. In order to determine whether TIGAR was upregulated in response to radiotherapy, U87MG cells were plated and 24 h later were irradiated with 2 or 4 Gy. To analyze protein expression, samples were collected 0.5, 4, 8 and 24 h and 0.5, 1, 2, 4, 8 and 24 h post-irradiation, respectively for 4 and 2 Gy. After 30 min of 4 Gy irradiation, a significant increase in TIGAR protein levels is observed, with levels returning to those of controls after 8 h. In 2 Gy irradiated cells, TIGAR induction was delayed and a clear increase can be observed 1 h after irradiation. Induction was still sustained 24 h after irradiation (Supplementary Fig. 3).

#### Clonogenic survival assay, DNA damage and SA- $\beta$ -Gal after TIGAR knockdown and radiotherapy

To determine the effects of TIGAR knockdown on U87MG cell radiosensitivity, clonogenic survival analysis was performed. In these studies, cells were transfected either with Neg-siRNA or TIGAR-siRNA 48 h prior to irradiation with 2, 4, 6, 8 and 10 Gy, and the surviving fraction was determined 14 days later. As shown in Fig. 2A, TIGAR knockdown decreased the clonogenic survival of

U87MG cells, reaching 50% cell death between 2 and 4 Gy, whereas control cells required doses between 4 and 6 Gy to achieve the same effect. TIGAR knockdown increased U87MG radiosensitivity with a dose enhancement factor at surviving fraction of 0.10 of 1.32.

U87MG cells were reseeded at low confluence 48 h after transfection (Neg and Tmix) and 14 days later SA- $\beta$ -Gal positive cells were quantified. A significant increase in senescence was observed in TIGAR-knockdown cells at basal condition and at low doses of radiation. Likewise, the combination of TIGAR-siRNA with 4 Gy of radiation caused the same levels of senescence obtained when treating negative control cells with as much as 8 Gy (Fig. 2B). Forty-eight hours after TIGAR knockdown, T98G cells were irradiated with 4 Gy, SA- $\beta$ -Gal positive cells were also quantified and a significant increase on senescent cells was observed in TIGAR-silenced cells versus control cells (Fig. 2C).

To further investigate the cellular processes through which TIGAR knockdown enhances radiosensitivity, we evaluated the induction of phosphorylated H2AX ( $\gamma$ -H2AX) nuclear foci, established as sensitive indicators of DNA double-strand breaks. The resolution of foci corresponded to double-strand breaks repair [29]. U87MG and T98G cells were transfected and then irradiated (4 Gy), and  $\gamma$ -H2AX foci were determined 30 min, 1, 4 and 24 h post-irradiation. As shown in Fig. 3A and B, TIGAR knockdown

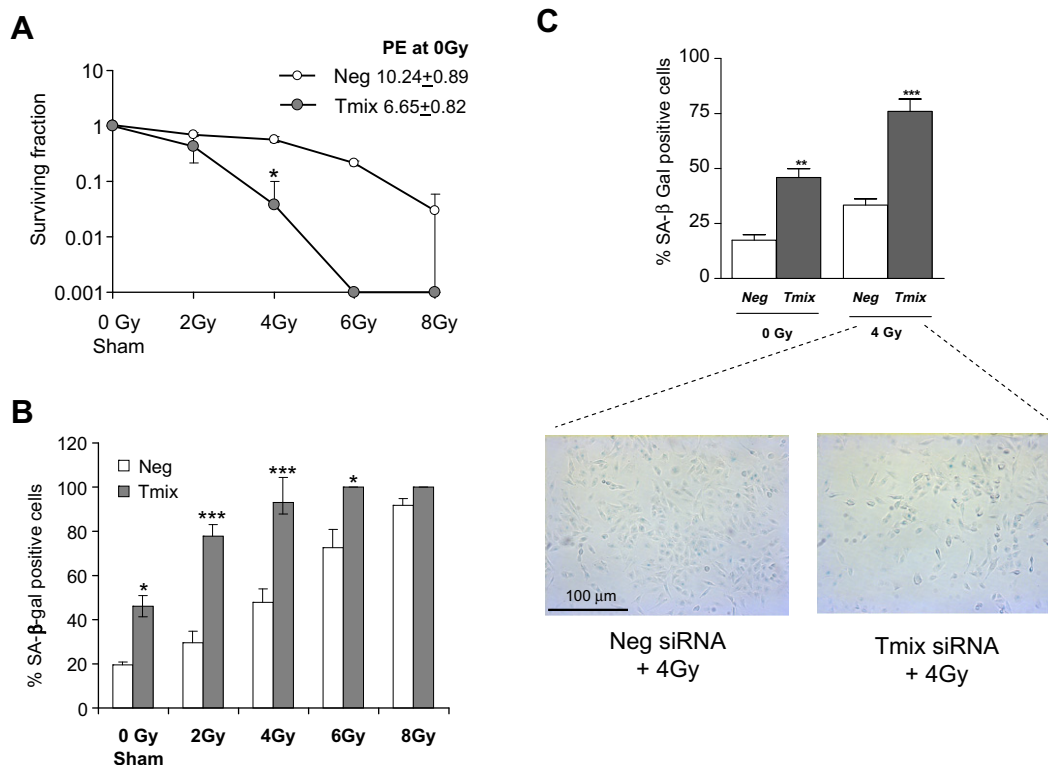


**Fig. 2.**  $\gamma$ -irradiation effects on TIGAR-knockdown U87MG cells. (A) Clonogenic survival of negative control or TIGAR-knockdown U87MG cells after a range of radiation doses (2–8 Gy). Each data point represents the mean  $\pm$  S.E.M. of three independent experiments. Student's *t* test versus the respective negative control values: \**p* < 0.05. (B) U87MG and (C) T98G cells. SA- $\beta$ -Gal activity was determined 14 days after negative (Neg) or TIGAR mix (Tmix) siRNAs transfection plus a range of radiation doses in U87MG cells and 4 Gy in T98G cells. Representative microscope images are shown in Fig. 2C. SA- $\beta$ -Gal positives cells were quantified by observation with bright-field microscopy at a magnification of 400 $\times$ . Data are means  $\pm$  S.E.M from at least three independent experiments. Student's *t* test versus the respective negative control values: \**p* < 0.05, \*\*\**p* < 0.001.

alone resulted in a significant increase in  $\gamma$ -H2AX foci when compared to the control (Negative siRNA). Radiation induced significant increases in the number of  $\gamma$ -H2AX foci at 30 min and 1 h, which progressively declined at 24 h. TIGAR silencing followed by 4 Gy resulted in an increase in the number of  $\gamma$ -H2AX foci significantly higher than that observed with radiation alone, thus suggesting the impact of TIGAR knockdown in the immediate DNA damage after irradiation. Of notice, 24 h after irradiation, the number of cells exhibiting  $\gamma$ -H2AX foci was higher with the combination treatment than with irradiation alone.

## Discussion

Glioblastoma is a highly lethal neoplasm with a median survival of 14.6 months [30]. Treatment is based on a multidisciplinary approach including surgery and adjuvant radiochemotherapy, and retreatment options have modest efficacy, improvements on current treatments are needed [31]. Despite efforts to understand the molecular pathogenesis of glioma, and the development of new therapies targeting signaling pathways with multitargeted kinase inhibitors or monoclonal antibodies aimed at increasing specificity and minimizing toxicity, the prognosis of patients with malignant glioma remains dismal. Therefore, new targets need to be uncovered. Cancer cells are usually under high oxidative stress compared with normal cells. Some authors have pointed out that introducing additional ROS insults by oxidative stress-generating agents or suppressing antioxidant capacity may selectively enhance cancer cell killing through stress overload or stress sensitization, whereas normal cells may be able to maintain redox homeostasis under exogenous ROS by adaptive response [32].

The aim of the present work was to determine the implication of TIGAR in glioma cell therapies. For this purpose, TIGAR was silenced in U87MG and T98G glioma cells and several metabolic parameters were analyzed. Significant increases in Fru-2,6-P<sub>2</sub> and lactate levels were observed in TIGAR-silenced U87MG cells 24 h post-transfection.

TIGAR has been described as a gene that is induced after moderate levels of stress, allowing the cells to repair gene damage and survive. Cellular metabolism releases low concentrations of ROS that can be compensated by cellular antioxidant mechanisms, one of them being TIGAR. Our results show that silencing TIGAR in basal conditions slightly increases (10%) ROS levels. A decrease in GSH levels was observed 24 h post-transfection that may be related with the slight increase in ROS levels observed at the same time point. Since oxidized glutathione (GSSG) was undetectable prior to and following siRNA transfection, only data for GSH concentration were plotted. Previously other authors have reported difficulty in measuring GSSG in several glioma cell lines [33]. We sought to investigate how TIGAR knockdown could affect cell growth. For this purpose, growth of U87MG and T98G cells was studied in a 7-day time-course by crystal violet staining. Cells transfected with TIGAR-siRNA showed a slope of growth significantly less steep than the control cells. As a consequence, cell number was noticeably lower versus control condition in both cell lines. On the whole, these results are in accordance with previous data regarding TIGAR as a novel p53 target gene that encodes a protein with similarity to the bisphosphatase domain of the bifunctional enzyme PFK-2/FBPase-2, one of the principal regulators of glycolysis [3]. Expression of TIGAR enhances the pentose phosphate pathway, hence conferring resistance to oxidative stress by enhancing NADPH production, which provides the necessary

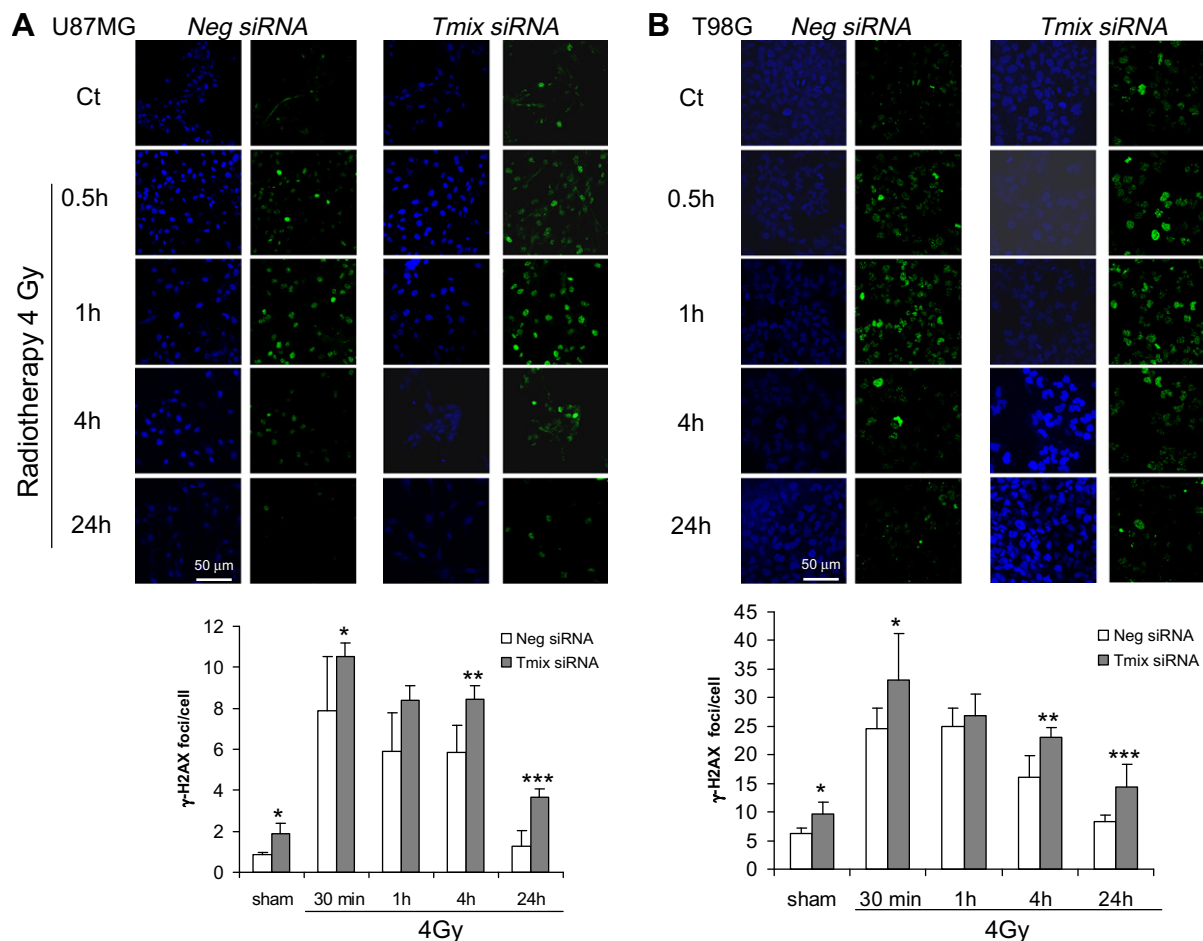


**Fig. 3.** Effect of TIGAR silencing on radiation-induced  $\gamma$ -H2AX foci in U87MG cells. Representative time course of  $\gamma$ -H2AX foci in U87MG (A) and T98G (B) cells irradiated with 4 Gy 48 h after transfection with negative (Neg) or TIGAR mix (Tmix) siRNAs. Green spots represent phosphorylated H2AX. Nuclei were stained using To-pro-3 dye (blue spots). Bars plotted in the lower panel represent the average number of foci/cell from three independent experiments as determined by the use of ImageJ software; at least 300 cells were counted from 10 randomly chosen fields of view. Data are means  $\pm$  S.E.M. Student's *t* test versus the respective negative control values: \*\**p* < 0.01, \*\*\**p* < 0.001.

reducing equivalents to restore GSH levels. Therefore, expression of TIGAR protects cells from both ROS and cell death, and TIGAR appears to belong to a group of p53-inducible genes that contribute to the survival of cells undergoing oxidative stress [1].

In order to find out whether the diminished cell number after TIGAR knockdown was due to cell death, different mechanisms were evaluated. We analyzed apoptosis in U87MG and T98G cells by annexin/PI staining and no significant differences were observed 48 h post-transfection. Recently, interest in autophagy (type II programmed cell death), has been renewed among oncologists, because different types of cancer cells undergo autophagy in response to anticancer therapies. Whether autophagy in cancer kills or protects cells is controversial [34]. In order to study autophagy, different proteins such as LC3 and p62 were analyzed by Western blot. No changes were observed in LC3 levels whereas p62 was slightly increased, indicating autophagy is not upregulated in U87MG cells. However, cell context is a key factor in determining the response of TIGAR to different stimuli, and Bensaad et al. have reported the ability of TIGAR to modulate the autophagic response in U2OS cells [5]. Senescence is a non-apoptotic mechanism often triggered in cancer cells and tissues in response to anti-cancer drugs [35]. In this sense, U87MG cells are known to show accelerated senescence after temozolomide [24,36] or camptothecin treatment [37]. Also a similar response has been described for T98G cells in response to temozolomide and etoposide [38]. TIGAR-silenced U87MG and T98G cells showed a significant increase

in SA- $\beta$ -Gal activity, although in other models, such as T-cell leukemia cells, overexpression of TIGAR has been related with a decrease in apoptosis and increase in senescence [6]. Premature senescence has been described as an emerging anticancer response elicited by different stresses, ROS among them [39]. This could be one of the mechanisms involved in the senescence induction caused by TIGAR knockdown and might explain the effect of TIGAR knockdown on cell growth. In addition, as ROS are known to induce DNA damage,  $\gamma$ -H2AX foci formation, an indicator of DNA double-strand breaks (DSBs) [40], was used to determine whether TIGAR silencing caused DNA damage through the action of ROS. The results showed that the number of foci per cell was significantly higher in TIGAR-silenced cells than in control cells 36 h after transfection, and BHA, a ROS scavenger, was able to decrease  $\gamma$ -H2AX foci to control levels in both U87MG and T98G cells.

Radiotherapy is a standard treatment for glioblastoma and new efforts aimed to increase effectivity, modulating radiation intensity and reducing adverse effects [41]. The results herein presented show that TIGAR knockdown increases lactate levels in U87MG cells while lowering GSH levels. The role of lactate in radiosensitization is unclear, but some authors point out that the increase in extracellular lactate might render cells more susceptible to irradiation [42], unlike those who claim that lactate contributes to radioresistance [43], emphasizing how interference with tumor cell metabolism may complement anticancer treatments [44]. Other studies have reported that decreases in GSH levels in response to

modifications of the glycolytic flux could enhance radiosensitivity of U87MG cells [45], supporting the results obtained in our study.

Recently a new anti-tumor molecule has been associated with the downregulation of TIGAR [19]. We have demonstrated that TIGAR is upregulated in U87MG glioblastoma cells after radiotherapy treatment. The increase in TIGAR protein levels could be observed very early after irradiation. In light of these data and taking into account that the expression of proteins like TIGAR might contribute to cancer cells' survival [17], this work proposes silencing TIGAR as a new target to enhance radiosensitivity in U87MG cells, a glioma cell model. Since tumoral cells are submitted to a high oxidative stress in comparison to normal tissue, which are able to maintain a steady-state balance of ROS levels [46], low side effects could be expected in non-tumoral cells, although more studies are needed in order to determine the effects of silencing TIGAR in normal tissue.

The response of cancer cells to radiation is determined by multiple molecular and cellular features. Glioma cells are highly resistant to the acute cytotoxic effects of radiation. Neither the U87MG nor the T98G cell lines demonstrated apoptosis in response to irradiation, but recently this effect could be obtained when irradiation was combined with Rapamycin [47]. In U87MG cells a 50% inhibition of colony formation required doses of 4–6 Gy, whereas only 2–4 Gy were required to achieve the same result in cells that had previously been silenced for TIGAR. Another anti-proliferative response in tumor cells is premature senescence, which is a phenotype that distinguishes tumor cells that survive drug exposure while losing the ability to form colonies from those that recover and proliferate after treatment [48]. Differences between senescence levels in irradiated U87MG cells and cells with the combined treatment were clear at low radiotherapy doses, while from 6 Gy onwards almost all the cells showed typical  $\beta$ -Gal positive activity and the characteristic enlarged and flattened morphology of senescent cells. Elucidation of the factors that regulate different aspects of treatment-induced senescence should help to improve the efficacy of cancer therapy [49]. An accelerated senescence response to fractionated radiation has been reported in U87MG cells; this effect is not so clear in p53 -mutant T98G cells [48]. Our results show that this senescent phenotype could be induced when the radiation was combined with TIGAR knockdown, and both cell lines, U87MG and T98G, had the same response, independent of their p53 status (Fig. 3A and B).

Finally, we evaluated DNA damage and repair in U87MG and T98G cells. Indeed, a critical event in determining radiosensitivity is the capacity to repair DSBs. In recent years,  $\gamma$ -H2AX expression has been established as a sensitive indicator of DSBs induced by clinically relevant doses of ionizing radiation [50,29]. At sites of radiation-induced DNA DSBs, the histone H2AX becomes rapidly phosphorylated ( $\gamma$ -H2AX) forming readily visible nuclear foci [51]. Basal number of foci vary between cell lines [52,53], as we noted for U87MG and T98G cells. Despite the different basal number of foci, our results showed a significant  $\gamma$ -H2AX foci increase in TIGAR-silenced cells, and this effect was enhanced when silencing was combined with radiation. Furthermore, the foci stayed longer, indicating this sensitization correlated with the delayed dispersion of phosphorylated histone H2AX foci (Fig. 3A and B). The maintenance of  $\gamma$ -H2AX foci levels, up to 24 h post-irradiation, suggests that TIGAR knockdown mediated radiosensitization involves the inhibition of DNA damage repair. This ability is essential for cell proliferation because maintaining DNA breaks can induce processes such as senescence.

In conclusion, this work aims to establish the “proof of principle” for novel targets in the treatment of glioma, taking advantage of TIGAR knockdown as a radiosensitizer. The present findings in glioma cells demonstrate that TIGAR knockdown inhibits cell proliferation and colony formation and suggests the implication of

ROS in the DNA repair impairment and senescence observed. Furthermore, TIGAR inhibition yields promising perspectives for further improvement of the radiotherapy of glioma and emphasizes the need for extended mechanistic studies.

### Conflict of interest statement

None declared.

### Acknowledgments

The authors would like to thank Dr. Josep Balart and technicians from the Applied Radiobiology and Experimental Radiotherapy Group from IDIBELL (ICO) for the use of irradiation facilities; Tom Yohannan for English editing; E. Adanero for her technical support; B. Torrejon from the Microscopy Unit, E. Castaño and E. Julià from the Cytometry Unit of the Scientific/Technical Service of the University of Barcelona (Bellvitge Campus), for excellent technical assistance and advice and A. Méndez and L. Novellademunt for his suggestions and helpful comments. This work was supported by the Ministerio de Ciencia y Tecnología (BFU 2009-07380) and Fondo de Investigación Sanitario (PI050689 and PI081085). Red Temática de Investigación Cooperativa en Cáncer/Instituto de Salud Carlos III (ISCIII), Spanish Ministry of Science and Innovation (ISCIII-RETICRD06/0020/0097), Fundación Medica Mútua Madrileña 2007, and Catalonia regional government (2009SGR395 and 2009SGR1059). M.A.P.R. and M.N.C.V. are recipients of scholarships from IDIBELL and the Ministerio de Educación, respectively.

### Appendix A. Supplementary data

Supplementary data associated with this article can be found, in the online version, at doi:10.1016/j.radonc.2011.07.002.

### References

- [1] Bensaad K, Tsuruta A, Selak MA, et al. TIGAR, a p53-inducible regulator of glycolysis and apoptosis. *Cell* 2006;126:107–20.
- [2] Li S, Ouellet H, Sherman DH, Podust LM. Analysis of transient and catalytic desosamine-binding pockets in cytochrome P-450 PkC from *Streptomyces venezuelae*. *J Biol Chem* 2009;284:5723–30.
- [3] Okar DA, Manzano A, Navarro-Sabate A, et al. PFK-2/FBPase-2: maker and breaker of the essential biofactor fructose-2,6-bisphosphate. *Trends Biochem Sci* 2001;26:30–5.
- [4] Obach M, Navarro-Sabate A, Caro J, et al. 6-Phosphofructo-2-kinase (pfkfb3) gene promoter contains hypoxia-inducible factor-1 binding sites necessary for transcription in response to hypoxia. *J Biol Chem* 2004;279:53562–70.
- [5] Bensaad K, Cheung EC, Vousden KH. Modulation of intracellular ROS levels by TIGAR controls autophagy. *Embo J* 2009;28:3015–26.
- [6] Hasegawa H, Yamada Y, Iha H, et al. Activation of p53 by Nutlin-3a, an antagonist of MDM2, induces apoptosis and cellular senescence in adult T-cell leukemia cells. *Leukemia* 2009;23:2090–101.
- [7] Martindale JL, Holbrook NJ. Cellular response to oxidative stress: signaling for suicide and survival. *J Cell Physiol* 2002;192:1–15.
- [8] Iida T, Furuta A, Kawashima M, et al. Accumulation of 8-oxo-2'-deoxyguanosine and increased expression of hMTH1 protein in brain tumors. *Neuro Oncol* 2001;3:73–81.
- [9] Barcellos-Hoff MH, Newcomb EW, Zagzag D, Narayana A. Therapeutic targets in malignant glioblastoma microenvironment. *Semin Radiat Oncol* 2009;19:163–70.
- [10] Adamson C, Kanu OO, Mehta AI, et al. Glioblastoma multiforme: a review of where we have been and where we are going. *Expert Opin Investig Drugs* 2009;18:1061–83.
- [11] Kanu OO, Hughes B, Di C, et al. Glioblastoma multiforme oncogenomics and signaling pathways. *Clin Med Oncol* 2009;3:39–52.
- [12] Sathornsumetee S, Reardon DA, Desjardins A, et al. Molecularly targeted therapy for malignant glioma. *Cancer* 2007;110:13–24.
- [13] Russo AL, Kwon HC, Burgan WE, et al. In vitro and in vivo radiosensitization of glioblastoma cells by the poly (ADP-ribose) polymerase inhibitor E7016. *Clin Cancer Res* 2009;15:607–12.
- [14] Blum R, Jacob-Hirsch J, Amariglio N, et al. Ras inhibition in glioblastoma down-regulates hypoxia-inducible factor-1alpha, causing glycolysis shutdown and cell death. *Cancer Res* 2005;65:999–1006.

- [15] Dewhirst MW, Cao Y, Moeller B. Cycling hypoxia and free radicals regulate angiogenesis and radiotherapy response. *Nat Rev Cancer* 2008;8:425–37.
- [16] King A, Gottlieb E. Glucose metabolism and programmed cell death: an evolutionary and mechanistic perspective. *Curr Opin Cell Biol* 2009;21:885–93.
- [17] Gottlieb E, Vousden KH. p53 regulation of metabolic pathways. *Cold Spring Harb Perspect Biol* 2010;2:a001040.
- [18] Chen EI, Hewel J, Krueger JS, et al. Adaptation of energy metabolism in breast cancer brain metastases. *Cancer Res* 2007;67:1472–86.
- [19] Lui VW, Lau CP, Cheung CS, et al. An RNA-directed nucleoside anti-metabolite, 1-(3-C-ethynyl-beta-d-ribo-pentofuranosyl)cytosine (ECyd), elicits antitumor effect via TP53-induced Glycolysis and Apoptosis Regulator (TIGAR) downregulation. *Biochem Pharmacol* 2010;79:1772–80.
- [20] Elbashir SM, Harborth J, Weber K, Tuschl T. Analysis of gene function in somatic mammalian cells using small interfering RNAs. *Methods* 2002;26:199–213.
- [21] Calvo MN, Bartrons R, Castano E, et al. PFKFB3 gene silencing decreases glycolysis, induces cell-cycle delay and inhibits anchorage-independent growth in HeLa cells. *FEBS Lett* 2006;580:3308–14.
- [22] Burnette WN. "Western blotting": electrophoretic transfer of proteins from sodium dodecyl sulfate-polyacrylamide gels to unmodified nitrocellulose and radiographic detection with antibody and radioiodinated protein A. *Anal Biochem* 1981;112:195–203.
- [23] Van Schaftingen E, Lederer B, Bartrons R, Hers HG. A kinetic study of pyrophosphate: fructose-6-phosphate phosphotransferase from potato tubers. Application to a microassay of fructose 2,6-bisphosphate. *Eur J Biochem* 1982;129:191–5.
- [24] Bergmeyer HU, editor. *Methods of enzymatic analysis*. p. 1464–8.
- [25] Senft AP, Dalton TP, Shertzer HG. Determining glutathione and glutathione disulfide using the fluorescence probe o-phthalaldehyde. *Anal Biochem* 2000;280:80–6.
- [26] Franken NA, Rodermond HM, Stap J, Haveman J, van Bree C. Clonogenic assay of cells in vitro. *Nat Protoc* 2006;1:2315–9.
- [27] Van Engeland LN M, Ramaekers FC, Schutte B, Reutelingsperger CP. Annexin V-affinity assay: a review on an apoptosis detection system based on phosphatidylserine exposure. *Cytometry* 1998;31:1–9.
- [28] Dimri GP, Lee X, Basile G, et al. A biomarker that identifies senescent human cells in culture and in aging skin in vivo. *Proc Natl Acad Sci USA* 1995;92:9363–7.
- [29] Rothkamm K, Kruger I, Thompson LH, Lobrich M. Pathways of DNA double-strand break repair during the mammalian cell cycle. *Mol Cell Biol* 2003;23:5706–15.
- [30] Krakstad C, Chekenya M. Survival signalling and apoptosis resistance in glioblastomas: opportunities for targeted therapeutics. *Mol Cancer* 2010;9:135.
- [31] Niyazi M, Siefert A, Schwarz SB, et al. Therapeutic options for recurrent malignant glioma. *Radiother Oncol* 2011;98:1–14.
- [32] Sun Y, St. Clair DK, Xu Y, Crooks PA, St. Clair WH. A NADPH oxidase-dependent redox signaling pathway mediates the selective radiosensitization effect of parthenolide in prostate cancer cells. *Cancer Res* 2010;70:2880–90.
- [33] Iida M, Sunaga S, Hirota N, et al. Effect of glutathione-modulating compounds on hydrogen-peroxide-induced cytotoxicity in human glioblastoma and glioma cell lines. *J Cancer Res Clin Oncol* 1997;123:619–22.
- [34] Zhuang W, Qin Z, Liang Z. The role of autophagy in sensitizing malignant glioma cells to radiation therapy. *Acta Biochim Biophys Sin (Shanghai)* 2009;41:341–51.
- [35] Singh R, George J, Shukla Y. Role of senescence and mitotic catastrophe in cancer therapy. *Cell Div* 2010;5:4.
- [36] Hirose Y, Katayama M, Mirzoeva OK, et al. Akt activation suppresses Chk2-mediated, methylating agent-induced G2 arrest and protects from temozolomide-induced mitotic catastrophe and cellular senescence. *Cancer Res* 2005;65:4861–9.
- [37] Morandi E, Severini C, Quercioli D, et al. Gene expression time-series analysis of camptothecin effects in U87-MG, DBTRG-05 glioblastoma cell lines. *Mol Cancer* 2008;7:66.
- [38] Sato Y, Kurose A, Ogawa A, et al. Diversity of DNA damage response of astrocytes and glioblastoma cell lines with various p53 status to treatment with etoposide and temozolomide. *Cancer Biol Ther* 2009;8:452–7.
- [39] Lu T, Finkel T. Free radicals and senescence. *Exp Cell Res* 2008;314:1918–22.
- [40] Zhou C, Li Z, Diao H, et al. DNA damage evaluated by gammaH2AX foci formation by a selective group of chemical/physical stressors. *Mutat Res* 2006;604:8–18.
- [41] Amelio D, Lorentini S, Schwarz M, Amichetti M. Intensity-modulated radiation therapy in newly diagnosed glioblastoma: a systematic review on clinical and technical issues. *Radiother Oncol* 2010;97:361–9.
- [42] Grotius J, Dittfeld C, Huether M, et al. Impact of exogenous lactate on survival and radioresponse of carcinoma cells in vitro. *Int J Radiat Biol* 2009;85:989–1001.
- [43] Sattler UG, Meyer SS, Quennet V, et al. Glycolytic metabolism and tumour response to fractionated irradiation. *Radiother Oncol* 2010;94:102–9.
- [44] Feron O. Pyruvate into lactate and back: from the Warburg effect to symbiotic energy fuel exchange in cancer cells. *Radiother Oncol* 2009;92:329–33.
- [45] Colen CB, Seraji-Bozorgzad N, Marples B, et al. Metabolic remodeling of malignant gliomas for enhanced sensitization during radiotherapy: an in vitro study. *Neurosurgery* 2006;59:1313–23 [discussion 1323–1314].
- [46] Dal-Pizzol F, Ritter C, Klamt F, et al. Modulation of oxidative stress in response to gamma-radiation in human glioma cell lines. *J Neurooncol* 2003;61:89–94.
- [47] Anandharaj A, Cinghu S, Park WY. Rapamycin-mediated mTOR inhibition attenuates survivin and sensitizes glioblastoma cells to radiation therapy. *Acta Biochim Biophys Sin (Shanghai)* 2011;43:292–300.
- [48] Quick QA, Gewirtz DA. An accelerated senescence response to radiation in wild-type p53 glioblastoma multiforme cells. *J Neurosurg* 2006;105:111–8.
- [49] Roninson IB, Broude EV, Chang BD. If not apoptosis, then what? Treatment-induced senescence and mitotic catastrophe in tumor cells. *Drug Resist Updat* 2001;4:303–13.
- [50] Rogakou EP, Pilch DR, Orr AH, Ivanova VS, Bonner WM. DNA double-stranded breaks induce histone H2AX phosphorylation on serine 139. *J Biol Chem* 1998;273:5858–68.
- [51] Sedelnikova OA, Rogakou EP, Panyutin IG, Bonner WM. Quantitative detection of (125)IdU-induced DNA double-strand breaks with gamma-H2AX antibody. *Radiat Res* 2002;158:486–92.
- [52] Short SC, Giampieri S, Worku M, et al. Rad51 inhibition is an effective means of targeting DNA repair in glioma models and CD133+ tumor-derived cells. *Neuro Oncol*; 13:487–9.
- [53] Burdak-Rothkamm S, Short SC, Folkard M, et al. ATR-dependent radiation-induced gamma H2AX foci in bystander primary human astrocytes and glioma cells. *Oncogene* 2007;26:993–1002.